

ANALYSIS OF ROBOTIC MACHINING OPERATIONS USING A RADIALY COMPLIANT END-EFFECTOR

Andrei Mario IVAN^{1,*}, Radu Constantin PARPALĂ², Cezara Georgia COMAN³

¹⁾²⁾³⁾ Lect. PhD. eng., MSP department, Politehnica University of Bucharest, Romania

Abstract: This paper presents a comparative analysis conducted by the authors in the field of robotic machining. The scope of the analysis was to compare light machining operations performed on various materials using an articulated-arm industrial robot equipped with a radially compliant end-effector. Thus, the experimental procedures were conducted on aluminium, wood and plastic. The approached machining operations were milling, chamfering and surface finishing. The goal of the research was to determine the values of the machining forces and to evaluate the influence of the end-effector compliance on machining results. The approach chosen for the experimental procedures was having the workpiece clamped on a dynamometer by using modular fixturing components. The equipment used for experimental purposes consisted of a six DOF articulated arm Kawasaki FS10E industrial robot with 10 kg. payload and a Kistler 9257B dynamometer for measuring the machining forces on three orthogonal directions corresponding to X, Y and Z axes of the part coordinate system. The robot was equipped with an ATI RC-340 radially compliant deburring tool. The robot programming method used during the experimental procedure was point to point block teaching using the teach pendant. The results were observed both visually and through the results shown by the Kistler dynamometer interface.

Key words: robotic milling, machining forces, chamfering, surface finishing, dynamometer, force measurement.

1. INTRODUCTION

Robotic machining applications are gaining more and more field in the industrial landscape. Even though the flexible manufacturing cells in which the industrial robot itself does the machining operations are not as widespread as welding or machine tending applications, an industrial robot has certain advantages which make it ideal for the most complex machining processes. One of the most desirable characteristics for an industrial robot integrated into a machining application is the ability to adapt to part shape variations and to compensate for its lack of accuracy. Thus, the research and development in the field of robotic machining focused in the last two decades towards adaptive trajectory planning and force feedback systems [1].

One of the elements that are particular to robotic machining systems are the compliant end-effectors, especially when compared to CNC machine tools. For a CNC milling centre, stiffness is always desirable. But an industrial robot, especially with a serial structure, is far less rigid than a machine tool, and it also has less accuracy [2]. A compliant end-effector, providing a controlled displacement of the tool either in axial or radial direction, ensures a constant and reliable contact with the part and

thus has an important role in following complex shapes and compensating for shape irregularities.

Although there is some variety regarding the operations that can be done with compliant end-effectors, traditionally the radially compliant tools are used for deburring applications and axially compliant tools for chamfering and drilling [3]. In order to expand the integration of compliant end-effectors in machining applications, a study on the influence of the compliance on machining results must be conducted.

The research presented by this paper continues the previous works of the authors in the field of robotic machining. While the experimental procedures conducted before focused on evaluating the influence of machining strategy and certain parameters (such as feeds and speeds) on manufacturing results, this research aims at using various materials to observe the influence of end-effector compliance. The materials used for the experimental procedures were aluminium, wood and plastic. The choice regarding the materials was made taking into consideration the available equipment, which was only capable of handling very light machining forces. Furthermore, the machining operations performed were also chosen in order to generate low force levels at the tool-workpiece interface: chamfering, surface finishing and – in order to test the limits of the experimental setup – milling [4]. The experimental results fall into two categories – those observed by visual inspection and the data acquired through the Kistler dynamometer interface.

* Corresponding author: 313 Splaiul Independentei,
Tel.: + 40-21-402 91 00;
Fax: -.
E-mail addresses: andrei.mario@yahoo.com (A. Ivan),
radu.parpala@gmail.com (R. Parpală), cezara.avram@yahoo.com
(C. Coman)



Fig. 1. Kawasaki FS10E articulated-arm robot and Kawasaki D controller.

2. EXPERIMENTAL EQUIPMENT

The experimental equipment used for acquiring the research data was based on light machining applications performed by a six degrees of freedom articulated arm industrial robot – Kawasaki FS10E, which is shown in Fig. 1. The Kawasaki FS10E industrial robot is controlled by a Kawasaki D controller.

The kinematic parameters of the Kawasaki FS10E industrial robot are described below [5]:

- No. of axes: 6.
- Joint limits
 - J1: $\pm 160^\circ$;
 - J2: $-105^\circ - 140^\circ$;
 - J3: $-155^\circ - 120^\circ$;
 - J4: $\pm 270^\circ$;
 - J5: $\pm 145^\circ$;
 - J6: $\pm 360^\circ$.
- Joint speeds
 - J1: 200 %/s;
 - J2: 140 %/s;
 - J3: 200 %/s;
 - J4: 360 %/s;
 - J5: 360 %/s;
 - J6: 600 %/s.

Also, taking into account the specific of the robotic applications performed during the experimental procedures, the payload and wrist loads should also be considered.

- Payload: 10 kg.
- Joint torques
 - J4: 21,5 N·m;
 - J5: 21,5 N·m;
 - J6: 9,8 N·m.
- Joint inertia
 - J4: 0,63 kg·m²;
 - J5: 0,63 kg·m²;
 - J6: 0,15 kg·m².


The Kawasaki FS10E industrial robot is equipped with an ATI QC41 automatic tool changer and an ATI RC340 radially compliant end-effector, which are shown in Fig. 2. The RC340 end-effector has a milling tool attached to the end of the spindle. The parameters of the milling tool are shown in Table 1.



Fig. 2. ATI RC340 radially compliant end-effector.

Table 1

Milling tool parameters

	Model	ATI 9150-RC-B-24065
	Tool diameter	9.525 mm (3/8")
	Length	15.875 mm (5/8")
	Shank diameter	6.35 mm (1/4")
	Materials	Aluminium, soft materials, plastics
	No. of teeth	6

The criteria regarding the choice of the milling tool revolves around the consideration that, for a reliable comparison between machining forces and results, the same tool was required for all operations, on all materials – aluminium, plastics and wood. Thus, the milling tool chosen for experimental procedures was a balanced one, suitable for all proposed operations. Also, for the experimental procedures, the following general machining parameters were used:

- Cutting speed $V_c = 167\text{--}227$ m/min;
- Feed/tooth $f_z = 0.014\text{--}0.031$ mm.

Considering the fact that the end-effector has a fixed spindle speed of 40000 rpm, the feed used for the experimental procedures were adjusted so that the feed/tooth was kept within the recommended range. This will lead to feed levels between 3360 mm/min and 7440 mm/min.

The parameters of the RC340 end-effector that are relevant for the research are presented below [6].

- Motor type: air turbine,
- Idle speed: 40 000 rpm,
- Max. Torque: 008 Nm,
- Power: 340 W,
- Weight: 1.2 kg,
- Compensation: max. ± 7.5 mm, recommended ± 3 mm,
- Compliance force: 12.7–42 N at 1–4.1 bar,
- Spindle air pressure: 6.2–6.5 bar,
- Collet size: 6 mm,

In order to acquire the required data for analysis – machining forces and torques at tool-workpiece interface – the parts were mounted on a Kistler 9257B dynamometer (shown in Fig. 3). The dynamometer is designed to be placed on a fixed support, with the part to be machined attached to it. Thus, it is suitable for the equipment used, as opposed to the solution in which the sensor is attached to robot's flange, because it does not place additional loads on robot's wrist – the payload of the Kawasaki FS10E industrial robot is 10 kg. Also, it does provide a stiff support for the workpiece. The Kistler dynamometer has a high resolution and is able to measure the values of the machining forces along three orthogonal axes, rela-

tive to the three axes (Ox , Oy and Oz) of the workpiece frame of reference, as well as the corresponding torques around the specified axes. As it can be seen from the dynamometer's parameters (shown in Table 2), it is more than capable of measuring the levels of machining forces for the proposed operations, being able to acquire values of up to 5 kN and measuring force values through four sensors and pressure-sensitive plates while maintaining the position of the workpiece [7].

In order to acquire the force and torque data, the information is sent through a signal amplifier (also shown in Fig. 3) to a computer with a suitable acquisition board. The computer displays the data and offers analysis tools and diagrams through a dedicated software interface.

The dynamometer was clamped to a T-slot table in front of the robot using modular fixture components. The workpiece was then placed on the top of the dynamometer using M8 screws.

3. EXPERIMENTAL RESULTS

In order to acquire the experimental data – both regarding the levels of machining force and torques and the results that were visually observed on the parts – multiple machining runs have been performed. For each run, the robot was programmed to follow a linear path, performing either a chamfering, lateral surface finishing or milling operation (Fig. 4). There were a total of eleven machining runs. The experimental setup is shown in Fig. 5.

As specified above, there were three type of materials included in the analysis – aluminium, plastic and wood. Depending on the observed behaviour of the system and the material during the experimental procedures, a number of four machining runs were performed on aluminium, five on plastic and two machining runs were performed on wood.



Fig. 3. The Kistler 9257B system: the dynamometer and the signal amplifier.

Table 2

Kistler 9257B parameters

Maximum values for measured forces	F_x, F_y, F_z	-5...5 kN
	F_z (for F_x and $F_y \leq 0.5 F_z$)	-5...10 kN
Overload	F_x, F_y, F_z	-7.5...7.5 kN
	F_z (for F_x and $F_y \leq 0.5 F_z$)	-7.5...15 kN
Threshold		< 0.01 N
Rigidity	C_x, C_y	> 1 kN/ μ m
	C_z	> 2 kN/ μ m
Natural frequency		3.5 kHz
Operating temperature		0...70 °C
Weight		7.3 kg
Clamping area		100×170 mm

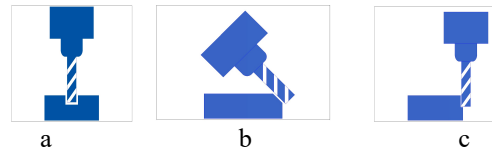


Fig. 4. Types of operations: a – slot milling; b – chamfering; c – lateral surface finishing.



Fig. 5. Experimental setup.



Fig. 6. Run 1 results.

Considering the above described concept, each of the eleven experimental runs are described below. All the experimental operations were conducted at a spindle

speed $n = 40\,000$ rpm. The maximum compliance force is of 42 N.

- **Run 1**

- Aluminium;
- $0.5 \times 45^\circ$ chamfering (type *b* operation – see Fig. 4);
- Conventional milling;
- Path length: 50 mm;
- Robot trajectory speed 100% – feed $V_f = 6800$ mm/min;
- *X* axis: max. value 34.58 N, median value 5.87 N;
- *Y* axis: max. value 52.76 N, median value 7.50 N;
- *Z* axis: max. value 32.90 N, median value 5.10 N;
- Observations: Medium surface quality, relatively constant spindle speed, very low tool deflection (see Fig. 6). The force levels were within robot specifications regarding load on arm and especially wrist loads. The highest machining forces were on the *Y* axis, corresponding to the feed direction. Also, the machining forces were below the maximum level at which the compliance system will cause the tool to depart from the programmed path, which means that the operation can be performed without compliance-related issues.
- Diagram shown in Fig. 11.

- **Run 2**

- Aluminium;
- $1 \times 45^\circ$ chamfering \times making a second pass from previous chamfering operation (type *b* operation – see Fig. 4);
- Conventional milling;
- Path length: 50 mm;
- Robot trajectory speed 100% – feed $V_f = 6800$ mm/min;
- *X* axis: max. value 17.49 N, median value 5.48 N;
- *Y* axis: max. value 22.52 N, median value 5.13 N;
- *Z* axis: max. value 35.80 N, median value 6.49 N;
- Observations: Medium surface quality, constant spindle speed, very low tool deflection. The results from Run 1 were confirmed, with largely the same behavior of the system – even if, in this case, the volume of the removed material was slightly larger.
- Diagram shown in Fig. 12.

- **Run 3**

- Aluminium;
- $0.5 \times 45^\circ$ chamfering (type *b* operation – see Fig. 4);
- Climb milling;
- Path length: 50 mm;
- Robot trajectory speed 100% – feed $V_f = 6800$ mm/min;
- *X* axis: max. value 39.00 N, mean value 10.03 N;
- *Y* axis: max. value 46.11 N, mean value 9.94 N;
- *Z* axis: max. value 27.07 N, mean value 9.11 N;
- Observations: Lower surface quality, variable spindle speed, spindle stalled after 20 mm. In this case, using the climb milling approach, the machining forces were at higher values than for the previous operations. Due to the characteristic engagement of the tool for climb machining, the relative lack of system rigidity (caused by both robot architecture and the compliance system) caused

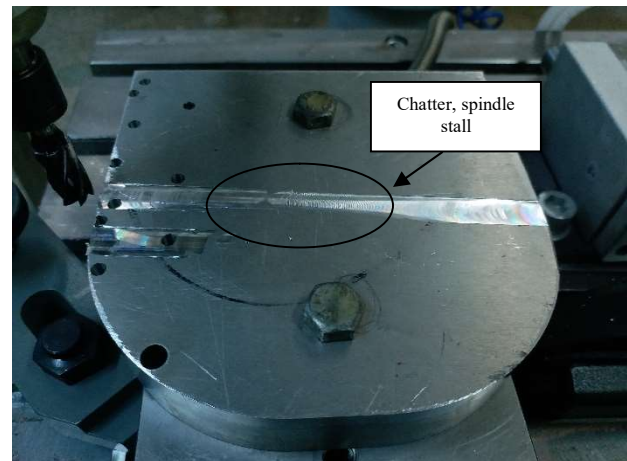


Fig. 7. Run 4 results.

lower surface quality. The force values exceeded both the level at which the compliance causes the tool to deflect and the allowable load on the spindle, which led to a stall.

- Diagram shown in Fig. 13.

- **Run 4**

- Aluminium;
- Milling, $a_e = 9.5$ mm, $a_p = 0.5$ mm (type *a* operation – see Fig. 4)
- Conventional milling;
- Path length: 50 mm;
- Robot trajectory speed 100% – feed $V_f = 6800$ mm/min;
- *X* axis: max. value 44.43 N, mean value 10.67 N;
- *Y* axis: max. value 50.87 N, mean value 10.92 N;
- *Z* axis: max. value 24.84 N, mean value 8.54 N;
- Observations: Good surface quality, variations in spindle speed, spindle stalled after 15 mm (see Fig. 7). Again, the machining forces proved to be at high values, causing the spindle to stop turning after 15 mm. The lower surface was of relatively good quality due to the machined surface being normal to the *Z* direction, which provides better rigidity. For the slot milling operation, the compliance system proved to be a major disadvantage, because teeth on both sides of the tool engaged the workpiece and generated chatter.
- Diagram shown in Fig. 14.

- **Run 5**

- Plastic;
- $0.5 \times 45^\circ$ chamfering (type *b* operation – see Fig. 4);
- Conventional milling;
- Path length: 50 mm;
- Robot trajectory speed 100% – feed $V_f = 6800$ mm/min;
- *X* axis: max. value 161.68 N, mean value 31.89 N;
- *Y* axis: max. value 88.71 N, mean value 13.56 N;
- *Z* axis: max. value 61.58 N, mean value 10.04 N;
- Observations: Less than average surface quality, constant spindle speed, some tool deflection. For this operation, the force were at higher values due to the plastic chips melting locally and sticking to the teeth. Because plastic is a softer material, it did not cause the spindle to stall, but caused significant tool deflection and, as a consequence,

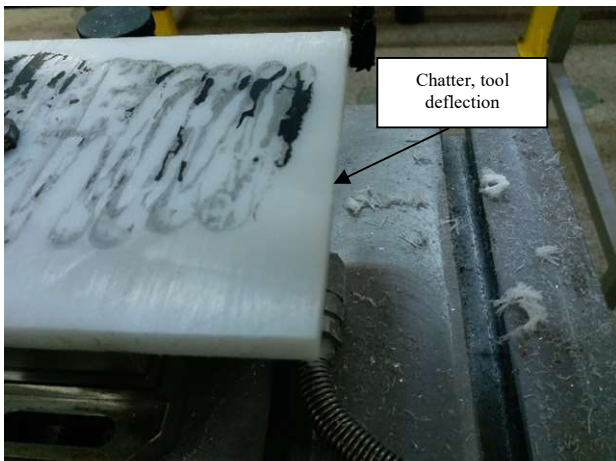


Fig. 8. Run 6 results.

poor surface quality. The tool deflection was caused by the force levels exceeding the level at which the compliance system causes the tool to deflect. The plastic operations were performed along the X axis, and thus the highest machining forces were on this direction.

- Diagram shown in Fig. 15.
- **Run 6**
 - Plastic;
 - Lateral surface finishing, $a_e = 0.5$ mm, $a_p = 8$ mm (type c operation – see Fig. 4);
 - Conventional milling;
 - Path length: 100 mm;
 - Robot trajectory speed 100%% – feed $V_f = 6800$ mm/min;
 - X axis: max. value 173.55 N, mean value 21.64 N;
 - Y axis: max. value 80.87 N, mean value 16.19 N;
 - Z axis: max. value 64.45 N, mean value 11.19 N;
 - Observations: Poor surface quality, constant spindle speed, significant tool deflection (see Fig. 8). These results largely confirmed the conclusions from the previous run, with relatively high machining force values, tool deflection due to the compliance system and, consequently, poor surface quality.
 - Diagram shown in Fig. 16.
- **Run 7**
 - Plastic;
 - Lateral surface finishing, $a_e = 0.5$ mm, $a_p = 8$ mm (type c operation – see Fig. 4);
 - Conventional milling;
 - Path length: 50 mm;
 - Robot trajectory speed 50% – feed $V_f = 3400$ mm/min;
 - X axis: max. value 144.96 N, mean value 19.17 N;
 - Y axis: max. value 75.59 N, mean value 12.96 N;
 - Z axis: max. value, 54.32 N mean value 8.98 N;
 - Observations: Poor surface quality, constant spindle speed, some tool deflection. The same operation as in the previous run was performed, with half the value of the feed. The force levels were somewhat reduced, but the results were largely the same. This confirmed that the issues were not caused by the feeds and speeds, but rather by the lack of system compliance and material characteristics.

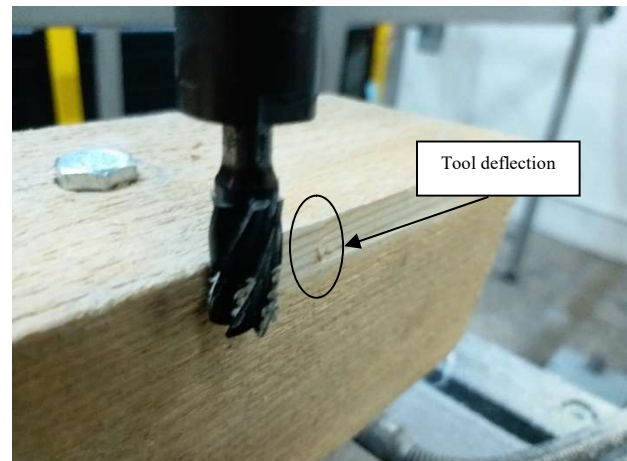


Fig. 9. Run 10 results.

- Diagram shown in Fig. 17.

- **Run 8**

- Plastic;
- Lateral surface finishing, following the same path as previous run and using the end-effector compliance to improve surface quality (type c operation – see Fig. 4).
- Conventional milling;
- Path length: 50 mm;
- Robot trajectory speed 50%% – feed $V_f = 3400$ mm/min;
- X axis: max. value 186.80 N, mean value 34.05 N;
- Y axis: max. value 108.28 N, mean value 17.35 N;
- Z axis: max. value 82.86 N, mean value 13.45 N;
- Observations: Medium surface quality, constant spindle speed, no tool deflection. Basically, the previous run was repeated with exactly the same parameters. Because the compliance works by applying a constant force to the workpiece, this pass was used as a finishing operation, in order to remove the material left from the previous run. The results showed that multiple passes with the same parameters (including the same robot path) using a radially compliant tool can improve the surface quality.
- Diagram shown in Fig. 18.

- **Run 9**

- Plastic;
- Lateral surface finishing, following the same path as previous run and using the end-effector compliance to improve surface quality (type c operation – see Fig. 4);
- Conventional milling;
- Path length: 50 mm;
- Robot trajectory speed 50%% – feed $V_f = 3400$ mm/min;
- X axis: max. value 50.29 N, mean value 11.85 N;
- Y axis: max. value 22.16 N, mean value 9.25 N;
- Z axis: max. value 32.07 N, mean value 7.53 N;
- Observations: Good surface quality, constant spindle speed, no tool deflection. The same operation from Run 7 and Run 8 was repeated and confirmed the previous results and conclusions.
- Diagram shown in Fig. 19.

- **Run 10**
 - Wood;
 - $0.5 \times 45^\circ$ chamfering (type *b* operation – see Fig. 4);
 - Conventional milling;
 - Path length: 50 mm;
 - Robot trajectory speed 50%% – feed $V_f = 3400$ mm/min;
 - X axis: max. value 90.06 N, mean value 22.42 N;
 - Y axis: max. value 103.85 N, mean value 14.89 N;
 - Z axis: max. value 74.95 N, mean value 12.06 N;
 - Observations: Good surface quality, variations in spindle speed, tool deflection (see Fig. 9). The operations performed on wood were done with the feed direction along the Y axis – this being the direction with the highest machining forces. The quality of the surface was good due to wood having good machinability characteristics, but the high force levels caused tool deflection and variations in spindle speed.
 - Diagram shown in Fig. 20.
- **Run 11**
 - Wood;
 - $1 \times 45^\circ$ chamfering – making a second pass from previous chamfering operation (type *b* operation – see Fig. 4);
 - Conventional milling;
 - Path length: 50 mm;
 - Robot trajectory speed 50%% – feed $V_f = 3400$ mm/min;
 - X axis: max. value 12.24 N, mean value 3.26 N;
 - Y axis: max. value 13.15 N, mean value 3.11 N;
 - Z axis: max. value 24.57 N, mean value 3.80 N;
 - Observations: Good surface quality, variations in spindle speed, spindle stalled after 25 mm. The second chamfering pass confirmed the observations from the previous run. The issues were caused by the very high spindle speed, which caused the wood to burn locally and hinder the cutting process, thus causing the spindle to stall after 25 mm.
 - Diagram shown in Fig. 21.

4. CONCLUSIONS

Taking into account that the end-effector has radial compliance, this provides some advantages, as well as some disadvantages. One of the disadvantages is linked to the fact that compliance is the opposite of rigidity.

Thus, depending on the forces at the tool-workpiece interface, the spindle may be deflected from the machined surface, if these forces exceed the levels corresponding to the set compliance value. The correspondence between the compliance and machining forces can be found by analyzing the diagrams in the end-effector documentation.

For aluminium machining experiments, chamfering operations using the conventional milling approach proved to be suitable for the setup that was used. If the chamfer does not require high precision levels and the part is properly aligned, with a suitable robot calibration the chamfering process can be done efficiently, especially with complex-shaped parts, where end-effector compliance can help following the outline of the workpiece. If necessary, the chamfering can be done using multiple passes, without significantly affecting the results.

Not the same aspects can be observed when using the climb milling approach. Given the climb milling nature, in which the chip is thicker at the tooth engagement and becomes thinner towards the end, this machining approach can generate more chatter and tool deflection if the setup does not provide a good stiffness, as observed in Run 3 (see Fig. 10). After several attempts, it has been concluded that climb milling cannot be used with this setup and these

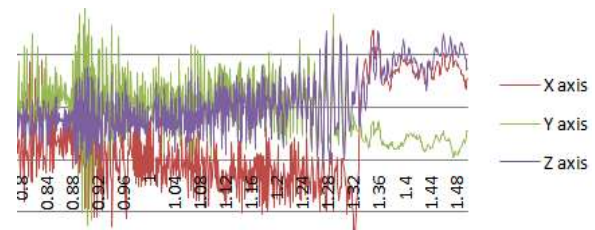


Fig. 10. Chatter and spindle stall in Run 3 (detail from Fig. 13).

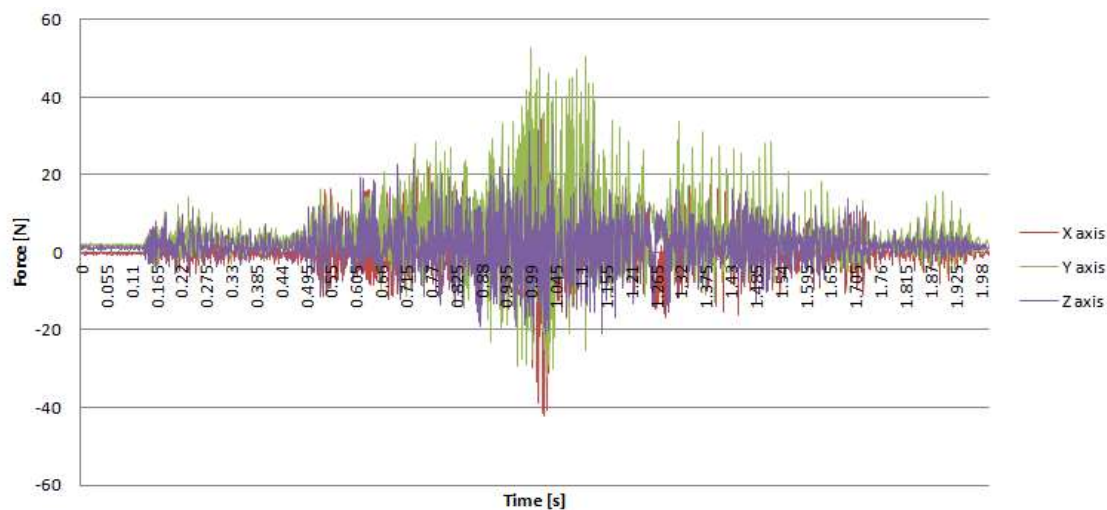


Fig. 11. Run 1 diagram.

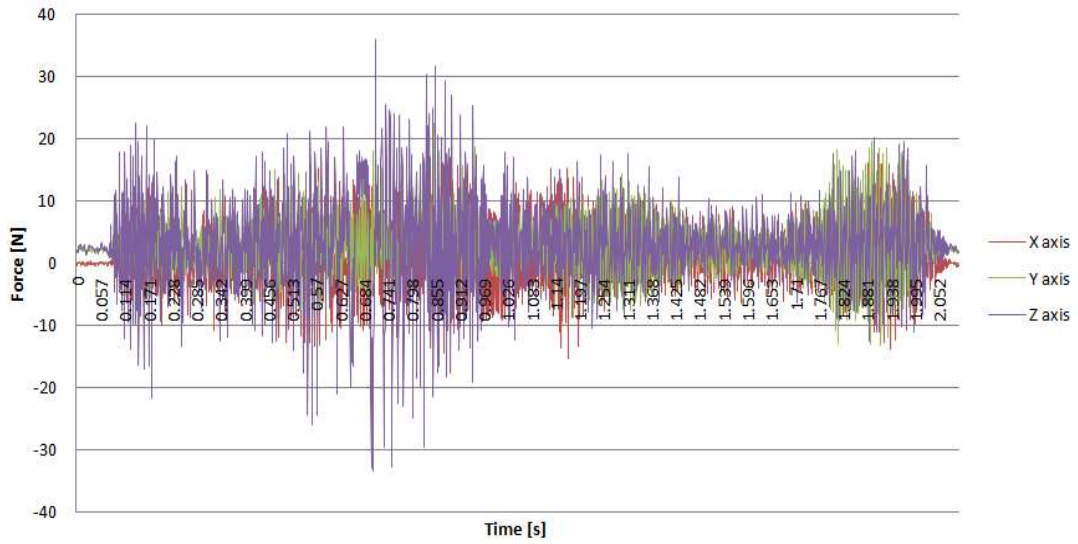


Fig. 12. Run 2 diagram.

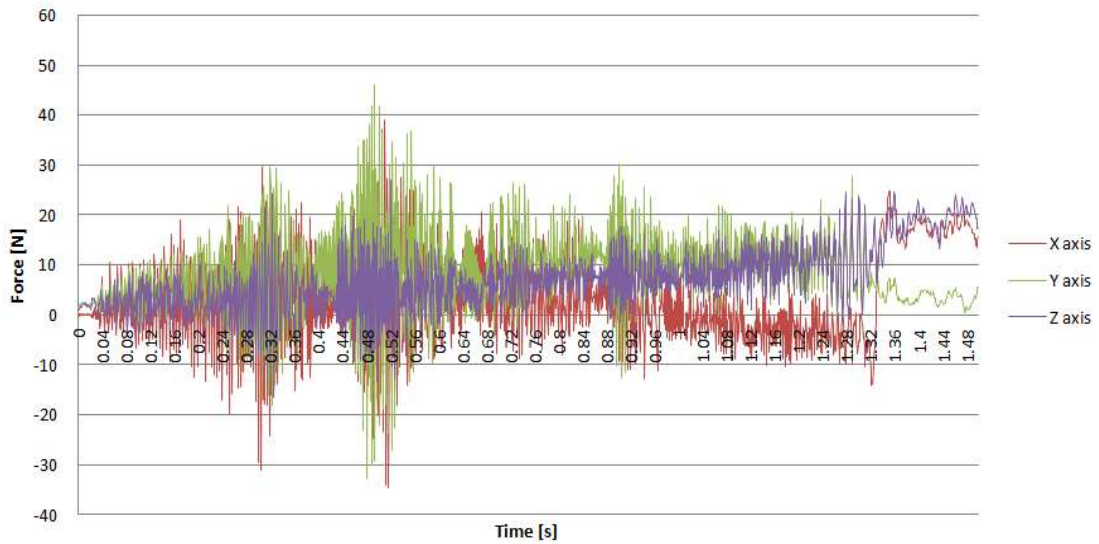


Fig. 13. Run 3 diagram.

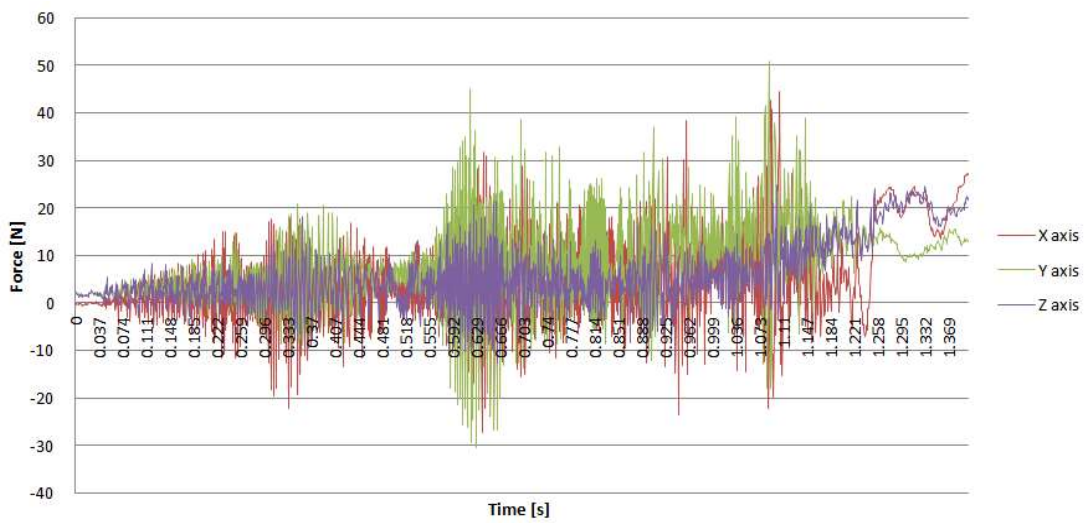


Fig. 14. Run 4 diagram.

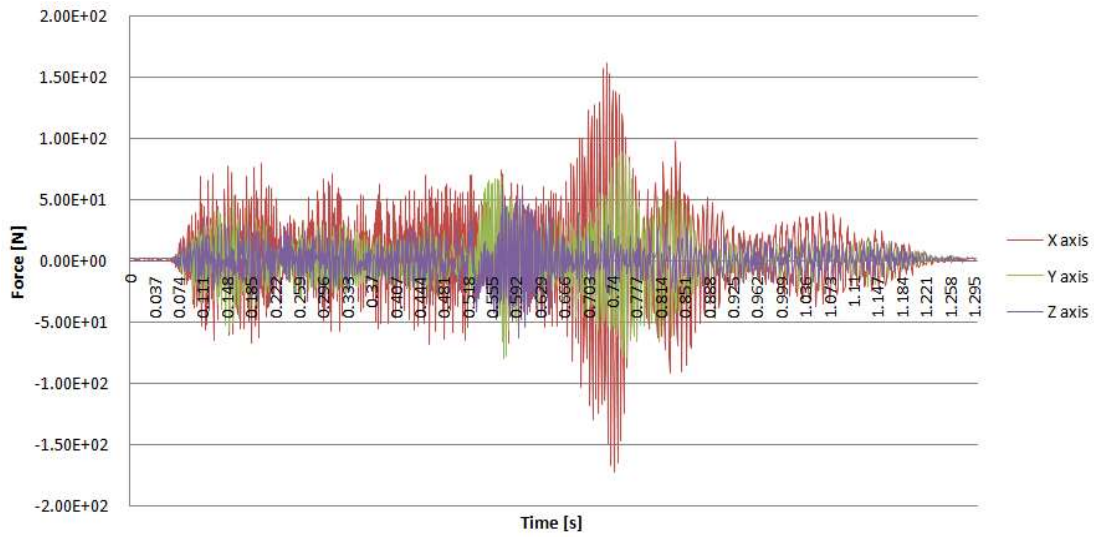


Fig. 15. Run 5 diagram.

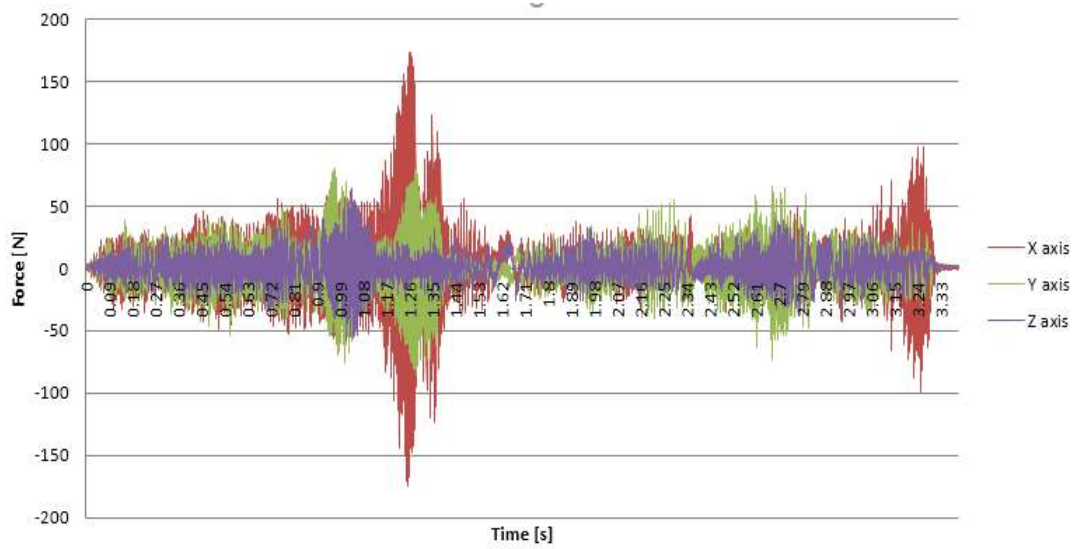


Fig. 16. Run 6 diagram.

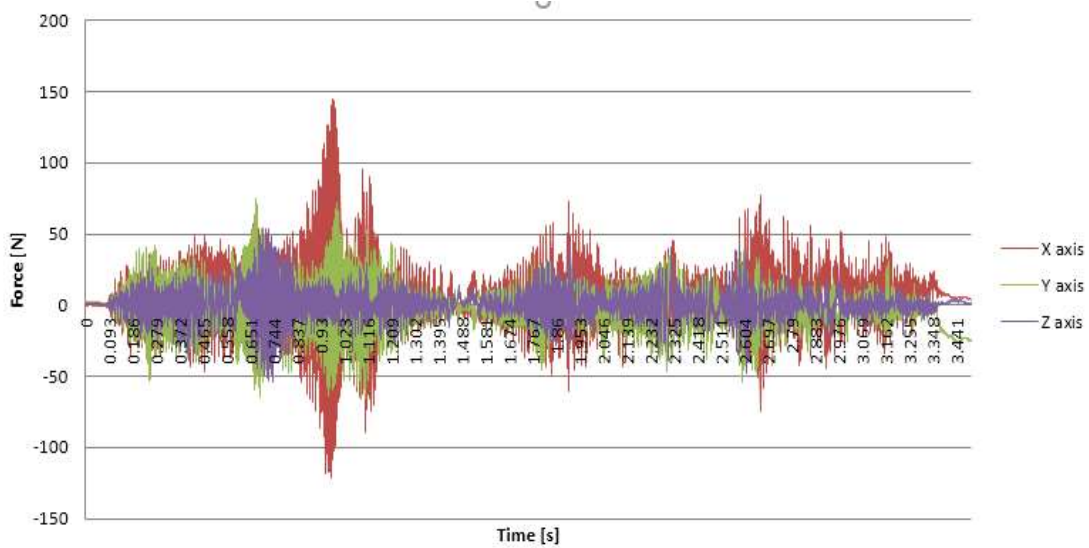


Fig. 17. Run 7 diagram.

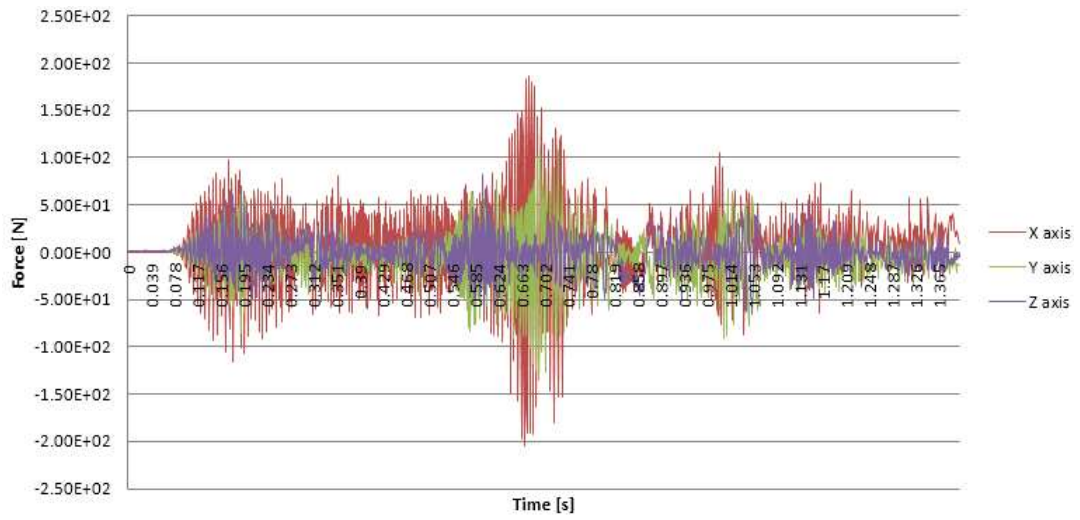


Fig. 18. Run 8 diagram.

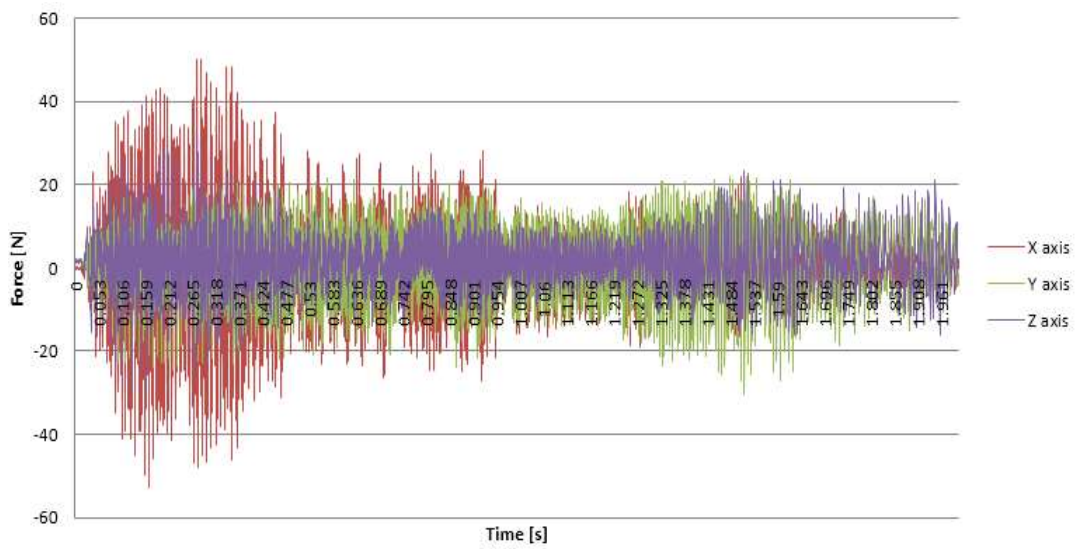


Fig. 19. Run 9 diagram.

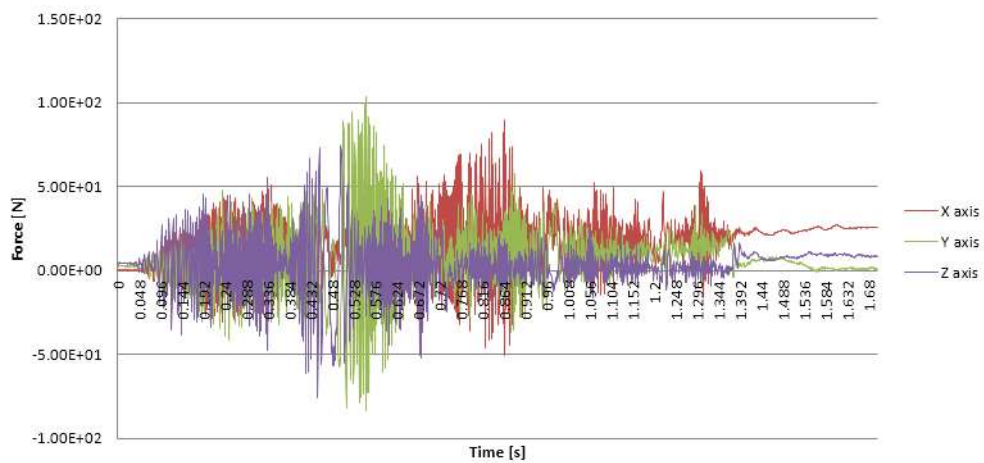


Fig. 20. Run 10 diagram.

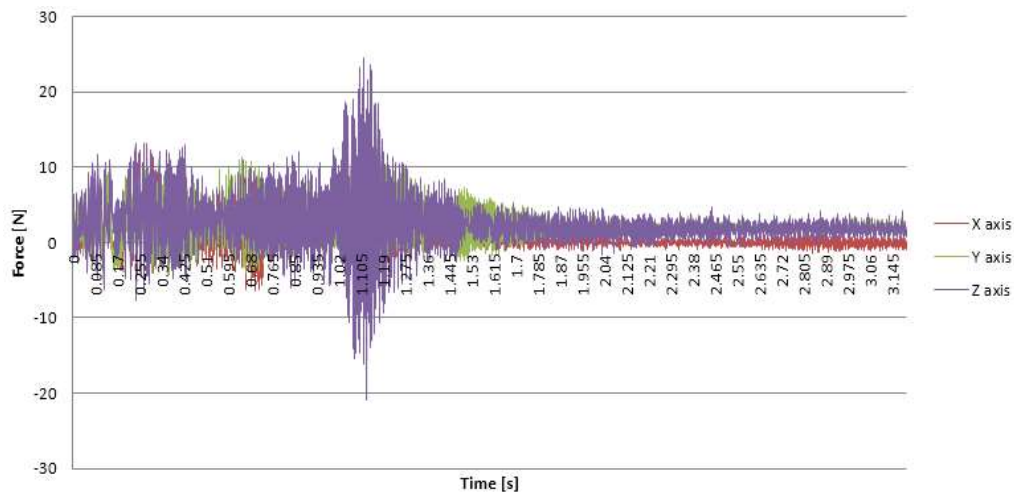


Fig. 21. Run 11 diagram.

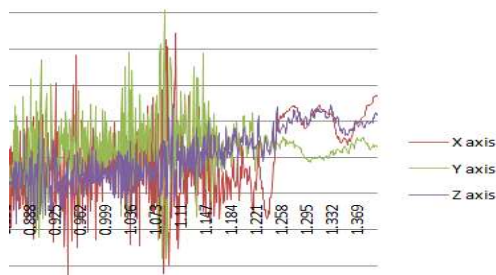


Fig. 22. Chatter and spindle stall in Run 4 (detail from Fig. 14).

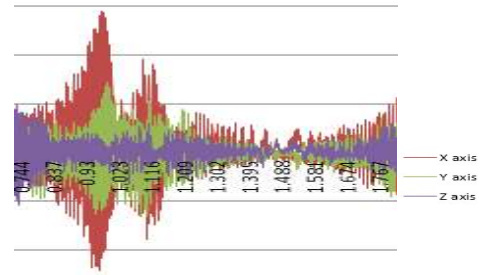


Fig. 23. Chatter in Run 7 (detail from Fig. 17).

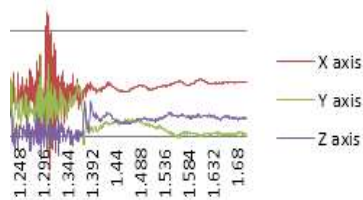


Fig. 24. Tool deflection in Run 10 (detail from Fig. 20).

Regarding Run 4, where a milling approach with full diameter engagement has been attempted and the results showed that radial compliance is not compatible with such engagement level. On one side, the torques generated even at 0.5 mm depth of cut are too high for the used end-effector and, on the other side, tool deflection from opposite directions generate too much chatter (Fig. 22).

For plastic, a material with a higher elasticity and also softer than aluminium, the tendency of the chips to stick to the milling tool teeth posed more problems. The quality of the machined surfaces is less than average, although chamfering can be done with satisfactory results, especially on harder plastics. Regarding lateral surface finishing, due to the high depth of cut, the end-effector compliance causes too much chatter and tool deflection (see Fig. 23). A better surface quality can be obtained with multiple passes, using the compliance to apply pressure on the part, but this approach is not productive, especially for a robotic application.

For wood, which has a higher tendency to stick to the tool teeth than plastic, the machining process is hindered after 20–25 mm and the tool losses proper engagement with the part (see Fig. 24). Here it should be noted that, with a harder, properly dried wood, it is possible to obtain better results.

ACKNOWLEDGEMENT: This work has been funded by University "Politehnica" of Bucharest, through the "Excellence Research Grants" Program, UPB – GEX 2017. Identifier: UPB- GEX2017, Ctr. No. 53/25.09.2017.

REFERENCES

- [1] I. Iglesias, M.A. Sebastián, J.E. Ares, *Overview of the State of Robotic Machining: Current Situation and Future Potential*, Procedia Engineering, Volume 132, 2015, pp. 911–917.
- [2] A. Nicolescu, *Roboți Industriali (Industrial Robots)*, Editura Didactică și Pedagogică, 2005.
- [3] A. Ivan, *Research regarding optimization of industrial robots for machining applications*, PhD Thesis, University "Politehnica" of Bucharest, 2011.
- [4] U. Schneider, M. Ansaloni, M. Drust, F. Leali, A. Verl, *Experimental Investigation of Sources of Error in Robot Machining*, Proc. WRSM 2013, International Conference Flexible Automation and Intelligent Manufacturing (FAIM), pp. 14–26, Porto, Portugal.
- [5] <https://robotics.kawasaki.com>, accessed: 2016-02-23.
- [6] <http://www.ati-ia.com/>, accessed: 2016-03-15.
- [7] <http://www.kistler.com>, accessed: 2011-08-12.